Electronic Supporting Information (ESI†) for

Synthesis of Heteronanostructures for Multimodality Biomedical Imaging-Guided Photothermal Therapy

Fengqin Xu[a,b], Xiaodong Li[c], Hongda Chen[a,b], Minghong Jian[a,b], Yanhong Sun[a,b],Guifeng Liu*[c], Lina Ma*[a], Zhenxin Wang*[a,b]

[a]State Key Laboratory of Electroanalytical Chemistry, Changchun Institute of Applied Chemistry, Chinese Academy of Sciences, Changchun, 130022, P. R. China.

[b]School of Applied Chemical Engineering, University of Science and Technology of China, Road Baohe District, Hefei, 230026, P. R. China.

[c]Department of Radiology China-Japan Union Hospital of Jilin University, Xiantai Street, Changchun, 130033, P. R. China.

*Corresponding Authors. E-mails: wangzx@ciac.ac.cn (ZW), malina@ciac.ac.cn (LM), and gfliu@jlu.edu.cn (GL)

Contents

1. Additional Experimental Section

Materials. Hydrogen tetrachloroaurate (III) trihydrate ($HAuCl_4 \cdot 3H_2O$), dopamine hydrochloride, ammonium hydroxide (28 wt% in water) and iron (III) chloride hexahydrate ($FeCl_3 \cdot 6H_2O$, 98%) were purchased from Alfa Aesar (Ward Hill, Massachusetts, USA). Polyoxyethylene (5) nonylphenyl ether (Igepal CO-520. average Mn 441), tert-butylamine-borane complex (TBAB, 97 %), Oleylamine (OAm, >70 %), 1-octadecene (ODE, 90%) and oleic acid (OA, 90%) were purchased from Sigma-Aldrich Co. (St. Louis, USA). Sodium oleate (95 %) was purchased from TCI (Tokyo, Japan). Poly (ethylene glycol) bis (3-aminopropyl) terminated (NH_2-PEG-NH_2) was purchased from Shanghai Ponsure Biological Technology Co., Ltd. (Shanghai, China). Diethylenetriaminepentacetic acid (DTPA) was received from Shanghai Aladdin Biochemical Technology Co., Ltd. (Shanghai, China). Gadolinium chloride ($GdCl_3 \cdot 6H_2O$, 99.99%) was purchased from Beijing HWRK Chem Co. Ltd (Beijing China). 3-(4,5-Dimethylthiazol-2-yl)-2,5-diphenyltetrazolium bromide (MTT) was received from Beijing Dingguo Biotechnology Ltd (Beijing, China). Calcein acetoxymethyl ester (Calcein AM) and propidium iodide (PI) were purchased from Dalian Meilun Biotechnology Ltd. (Dalian, China). The culture medium Leibovitz's L-15 and DMEM were purchased from Jiangsu KeyGEN BioTECH Co. Ltd. (Jiangsu, China). Fetal bovine serum (FBS) was purchased from Gibco Co. (New York, USA). MDA-MB-231 cell lines were purchased from Shanghai Cell Bank, CAS (Shanghai, China). The other reagents were obtained from Beijing Chemical Reagents Company (Beijing, China). BALB/c nude mice (females) were purchased from Vital River

Company (Beijing, China). All chemicals were analytical grade and used as received without further purification. Milli-Q water (18.2 MΩ cm) was used in all experiments.

Characterization. High-magnification transmission electron microscope (HRTEM) micrographs were obtained on a FEI Tecnai G2S-Twin TEM (FEI Co., USA) with a field emission gun operating at 200 kV. Fourier transform infrared (FTIR) spectra were captured with a Bruker Vertex 70 spectrometer. The X-ray photoelectron spectroscopy (XPS) measurements were conducted with a VG ESCALAB MKII spectrometer (VG Scientific Ltd., UK). All hydrodynamic diameter and Zeta potential measurements were carried out on Malvern Zetasizer Nano ZS (Malvern Instruments Ltd., UK). ELAN 9000/DRC inductively coupled plasma mass spectrometry (ICP-MS) system (Perkin Elmer, USA) was used for analyzing the elements in samples. The MTT assay was measured using a Versamax microplate reader (Bio-Tek Instruments, Inc., USA). The T_1-weighted MRI images and T_2-weighted MRI images were acquired using a 3.0 T clinical MRI scanner (Philips) with the following imaging parameters: T_2 MR imaging parameters, repetition time (TR), 4000 ms; echo time (TE), 84 ms; field of view, 102 mm × 72 mm; and slice thickness, 2.0 mm. T_1 MR imaging parameters, repetition time (TR), 240 ms; echo time (TE), 15.9 ms; field of view, 120 mm × 72 mm; and slice thickness, 2.0 mm. The CT images were acquired using a 64-detector row CT unit (General Electric Co., Milwaukee, WI, U.S.) with the following parameters: thickness, 0.6 mm; pitch, 0.99; 120 kVp, 300 mA; field of view, 103 mm; gantry rotation time, 0.5 s; table speed, 15.9 mm s^{-1}.

Synthesis of Au Seeds. The Au seeds with diameter of 5 nm were prepared using

previously reported procedure with slight modifications [1]. Briefly, 0.1 mmol $HAuCl_4 \cdot 3H_2O$, 4 mL of OAm and 4 mL of cyclohexane were mixed and magnetically stirred at the desired temperature of 10 ℃ under a gentle stream of high purity argon gas to form the precursor solution. 0.2 mmol TBAB complex was dissolved in 0.4 mL of OAm and 0.4 mL of cyclohexane, and then injected into the precursor solution. The color of solution changed to deep red immediately after the injection of TBAB complex solution. After the mixture was aged for 40 min, the Au seeds were precipitated by addition of 30 mL of ethanol and centrifugation at 8,000 rpm for 8 min. The final products were re-dispersed in hexane for use.

Synthesis of Au-Fe_3O_4 NPs. Iron-oleate complex ($Fe(OL)_3$) was first obtained by dissolving ferric chloride and sodium oleate in a mixture containing ethanol, water and hexane [2, 3]. After reaction at 70 ℃ for 4 h, the resulting solution was washed with deionized water for three times. The Au-based dumbbell-like NPs (DBNPs) were prepared by mixing 0.5 mmol OA, 0.5 mmol OAm, 1 mmol $Fe(OL)_3$, and 0.1 mmol Au colloids in hexane into 5 mL of ODE. The solution was heated to 110 ℃ for 20 min to remove hexane and then refluxed for 30 min at 310 ℃.[4] After the reaction, the solution was cooled down to room temperature and the Au-Fe_3O_4 NPs were harvested by adding 30 mL of ethanol followed by centrifugation at 7,500 rpm for 10 min. The resultant NPs were then re-dispersed in hexane.

Tumor Models. 2×10^6 MDA-MB-231 cells suspended in 100 μL of serum free cell medium were inoculated subcutaneously in several female BALB/c mice. The mice were used for further experiments when the tumor had grown to 3-4 mm in diameter.

***In vivo* Toxicity Studies.** Healthy BALB/c mice were intravenously administered with 100 μL of NaCl solution (0.9 wt%) containing 2 mg mL^{-1} Au-Fe_3O_4@PDA-PEG-DTPA-Gd or Au-Fe_3O_4@PDA-PEG. Several other mice were intravenously administered with 100 μL of 0.9% NaCl solution as the controls. Over one month period, the mice were observed for behavioral changes and weights were monitored. Then, the mice were sacrificed and the blood was collected for hematology analysis. Several organs including heart, liver, lung, kidney, and spleen were fixed in 4% paraformaldehyde to stain with hematoxylin and eosin (H&E) for histopathology analysis.

2. Additional Figures S1-S14.

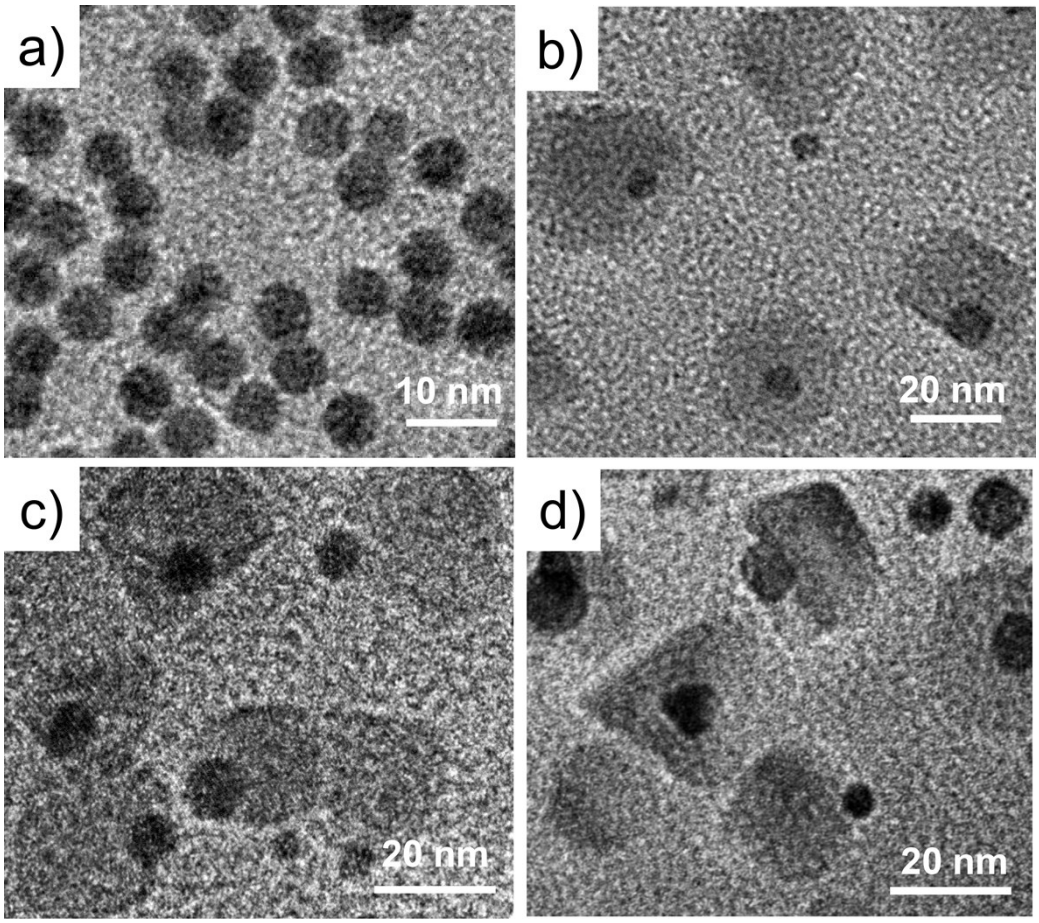

Fig. S1. TEM micrographs of (a) Au NPs, (b) Au-Fe_3O_4 heterodimerics, (c) Au-Fe_3O_4@PDA, and (d) Au-Fe_3O_4@PDA-PEG, respectively.

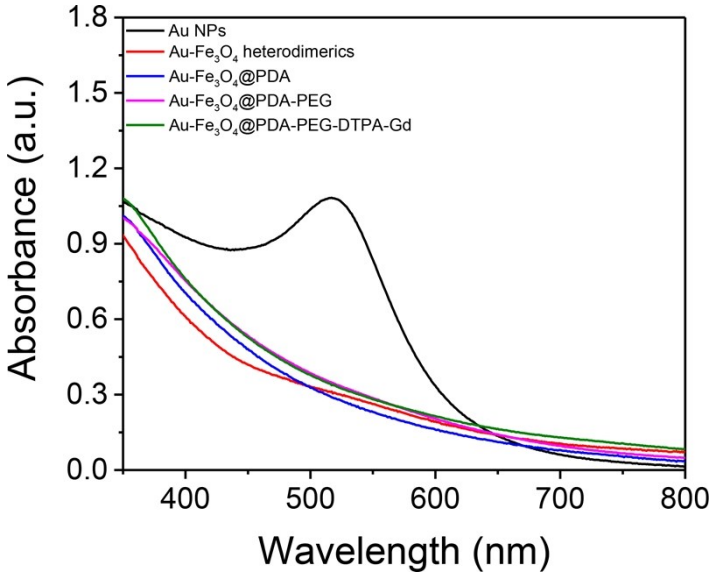

Fig. S2. UV-Visbile spectra of Au NPs, Au-Fe_3O_4 heterodimerics, Au-Fe_3O_4@PDA, Au-Fe_3O_4@PDA-PEG and Au-Fe_3O_4@PDA-PEG-DTPA-Gd, respectively.

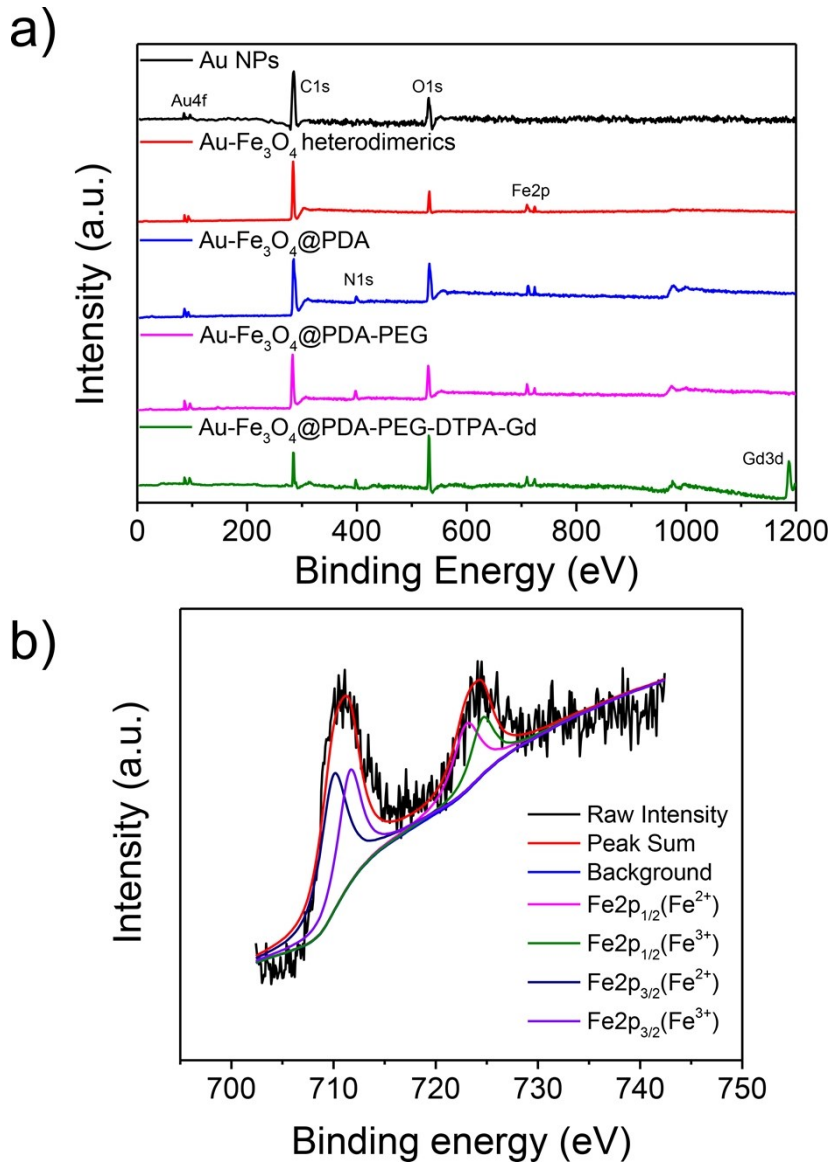

Figure S3. XPS spectra of (a) the as-synthesized Au NPs, Au-Fe_3O_4 heterodimerics, Au-Fe_3O_4@PDA, Au-Fe_3O_4@PDA-PEG and Au-Fe_3O_4@PDA-PEG-DTPA-Gd, respectively. (b) XPS spectrum of Fe2p of Au-Fe_3O_4 heterodimerics.

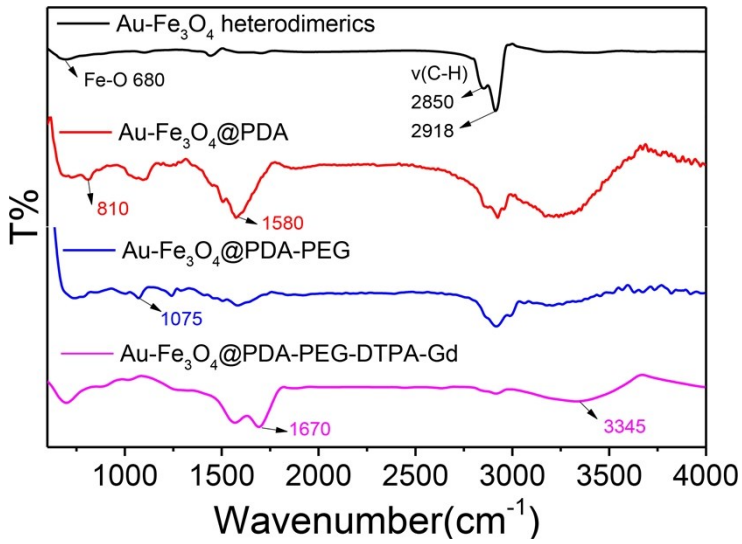

Figure S4. FTIR spectra of Au-Fe_3O_4 heterodimerics, Au-Fe_3O_4@PDA, Au-Fe_3O_4@PDA-PEG and Au-Fe_3O_4@PDA-PEG-DTPA-Gd, respectively.

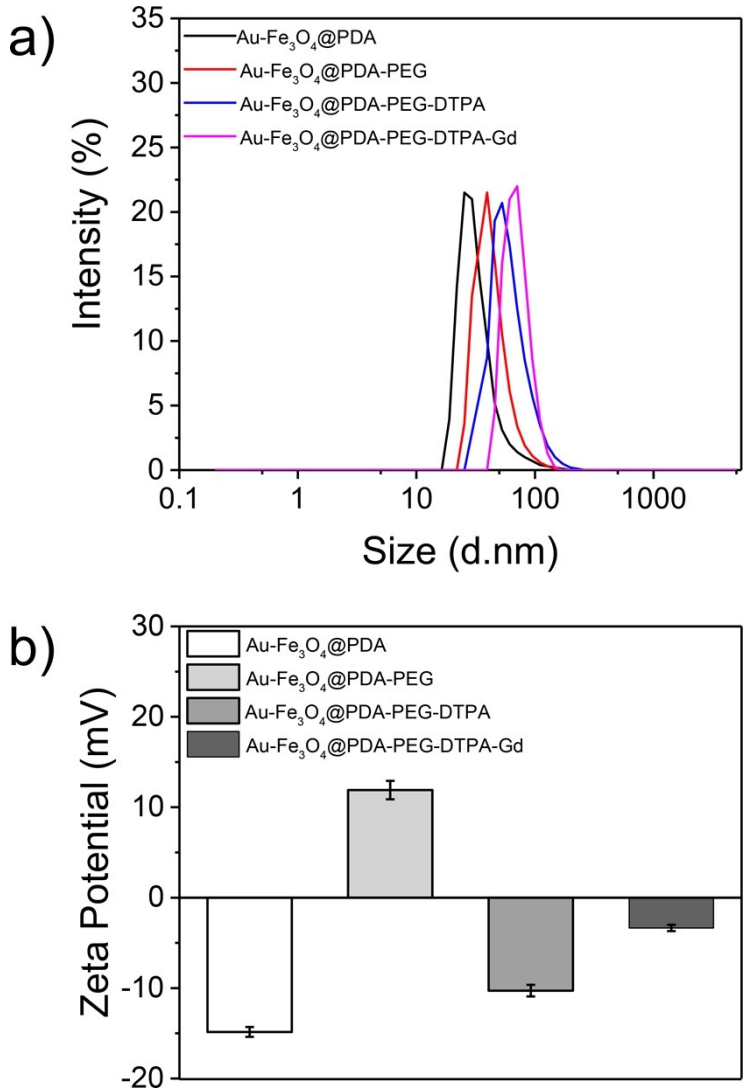

Figure S5. (a) Hydrodynamic (HD) sizes and (b) Zeta potentials of Au-Fe_3O_4@PDA, Au-Fe_3O_4@PDA-PEG, Au-Fe_3O_4@PDA-PEG-DTPA and Au-Fe_3O_4@PDA-PEG-DTPA-Gd, respectively.

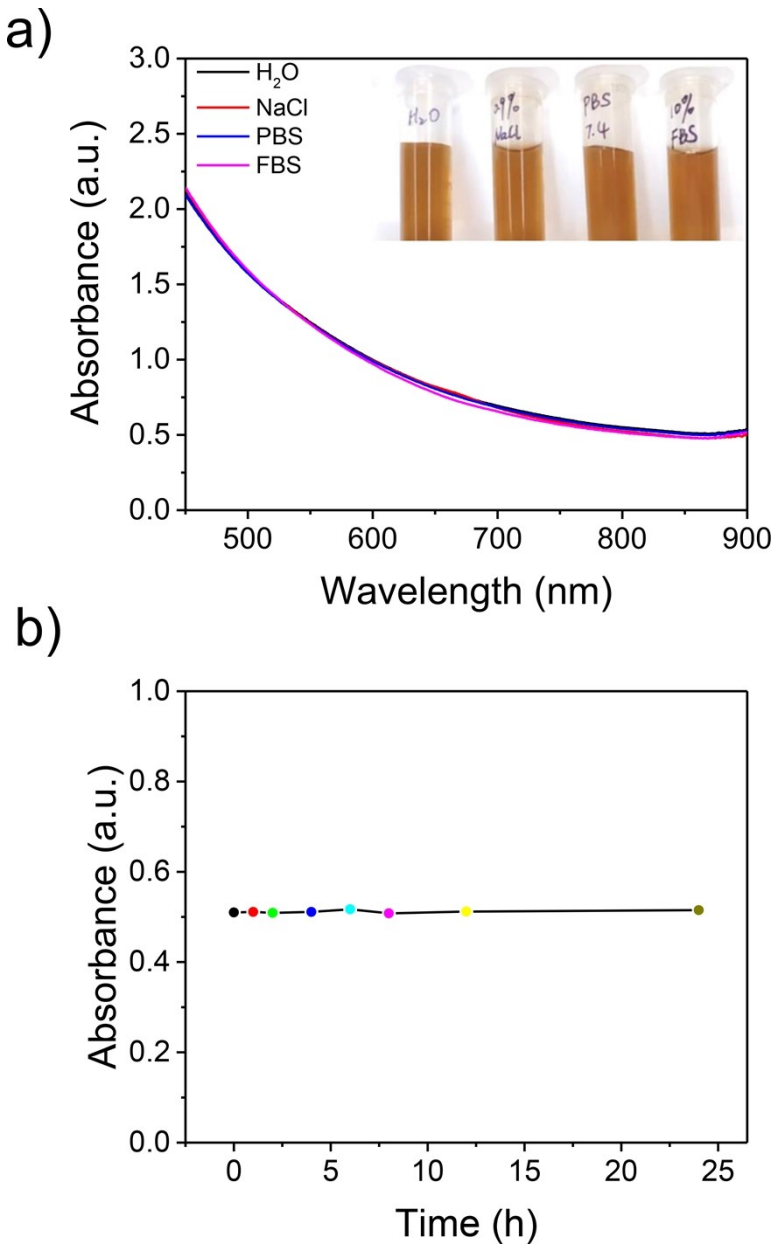

Figure S6. (a) UV-visible spectra of Au-Fe_3O_4@PDA-PEG-DTPA-Gd in H_2O, 0.9 wt% NaCl solution, PBS (pH=7.4), and 10% serum, respectively. Inset represents the corresponding photographs of Au-Fe_3O_4@PDA-PEG-DTPA-Gd solutions. (b) The absorbance of Au-Fe_3O_4@PDA-PEG-DTPA-Gd in 10% serum at 808 nm as a function of the incubation time.

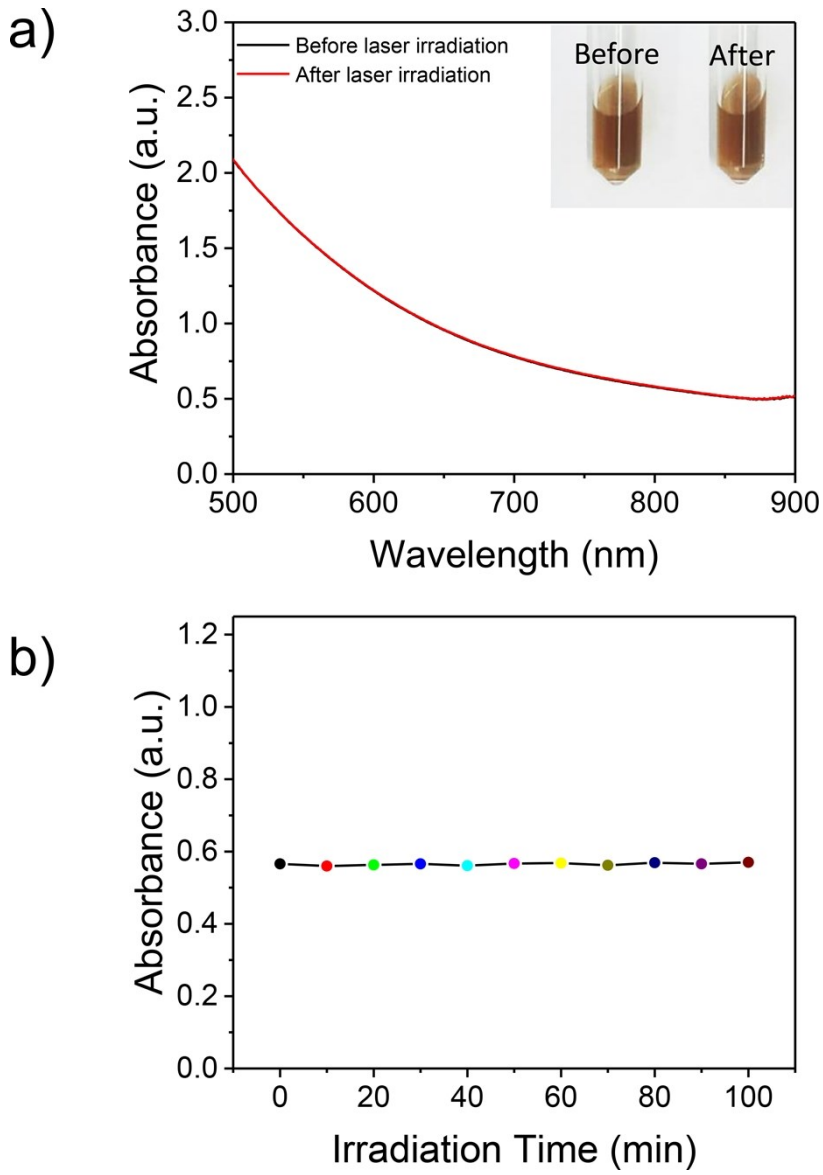

Figure S7. (a) UV-visible absorption spectra of Au-Fe_3O_4@PDA-PEG-DTPA-Gd dispersed in water before and after 808 nm NIR laser irradiation for 100 min (1.36 W cm^{-2}). The inset shows the corresponding photographs of Au-Fe_3O_4@PDA-PEG-DTPA-Gd before and after 808 nm NIR irradiation. (b) The absorbance of Au-Fe_3O_4@PDA-PEG-DTPA-Gd at 808 nm as a function of the irradiation time.

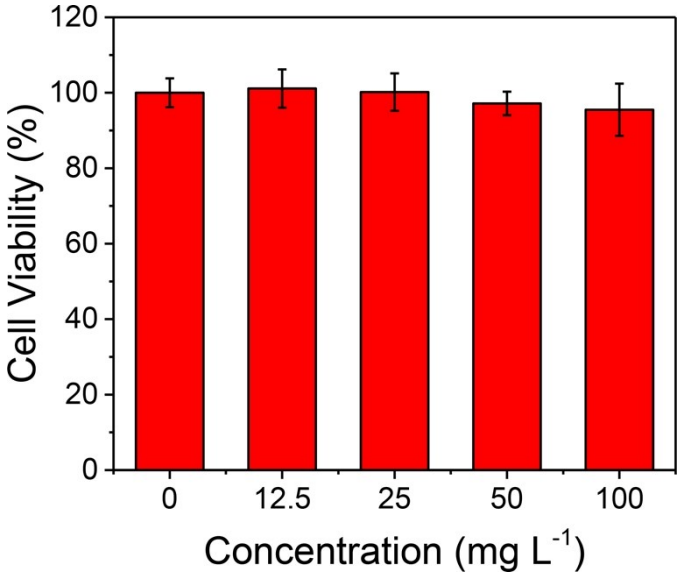

Fig. S8. Cell viabilities of HUVEC cells incubated with various concentrations of Au-Fe_3O_4@PDA-PEG-DTPA-Gd (Gd content: 0-100 mg L^{-1}).

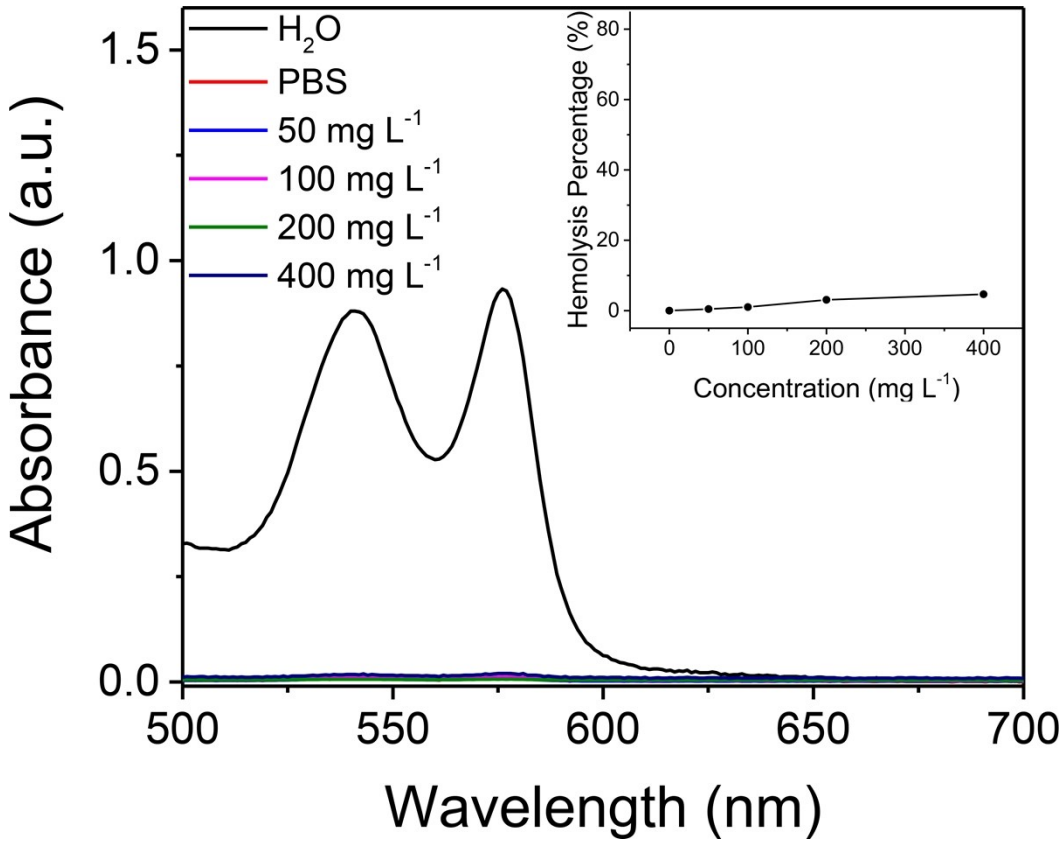

Figure S9. Hemolysis assay of Au-Fe_3O_4@PDA-PEG-DTPA-Gd. The PBS is used as negative control while H_2O is used as positive control, respectively. Inset illustrates the hemolysis percentage with different concentrations of Au-Fe_3O_4@PDA-PEG-DTPA-Gd (50, 100, 200 and 400 mg L^{-1}).

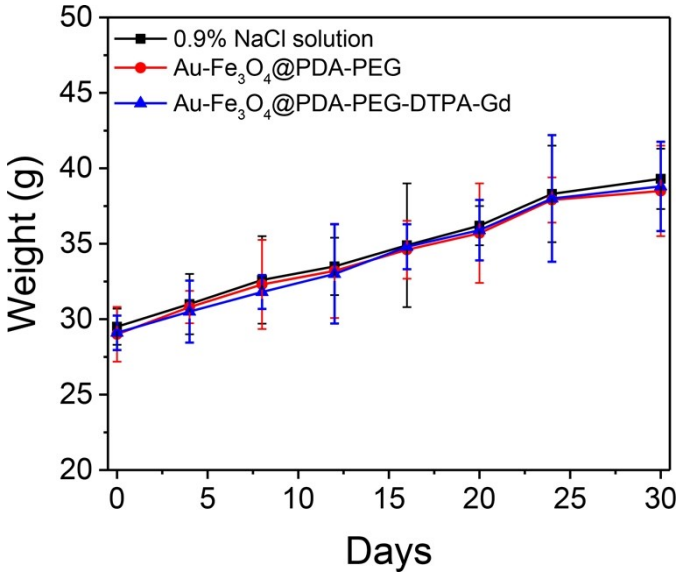

Figure S10. Bodyweight curves of health mice treated with 0.9% NaCl solution, Au-Fe_3O_4@PDA-PEG and Au-Fe_3O_4@PDA-PEG-DTPA-Gd, respectively. Error bars mean standard deviations (n=3).

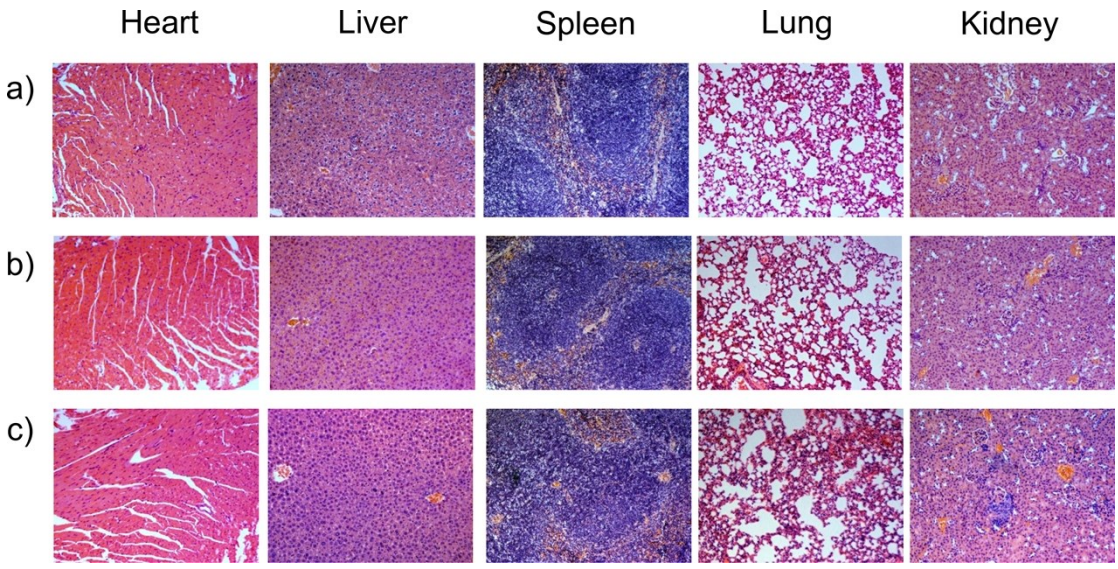

Figure S11. H&E staining of major organs from health mice treated with (a) 0.9% NaCl solution, (b) Au-Fe_3O_4@PDA-PEG and (c) Au-Fe_3O_4@PDA-PEG-DTPA-Gd at 30 days post-injection, respectively.

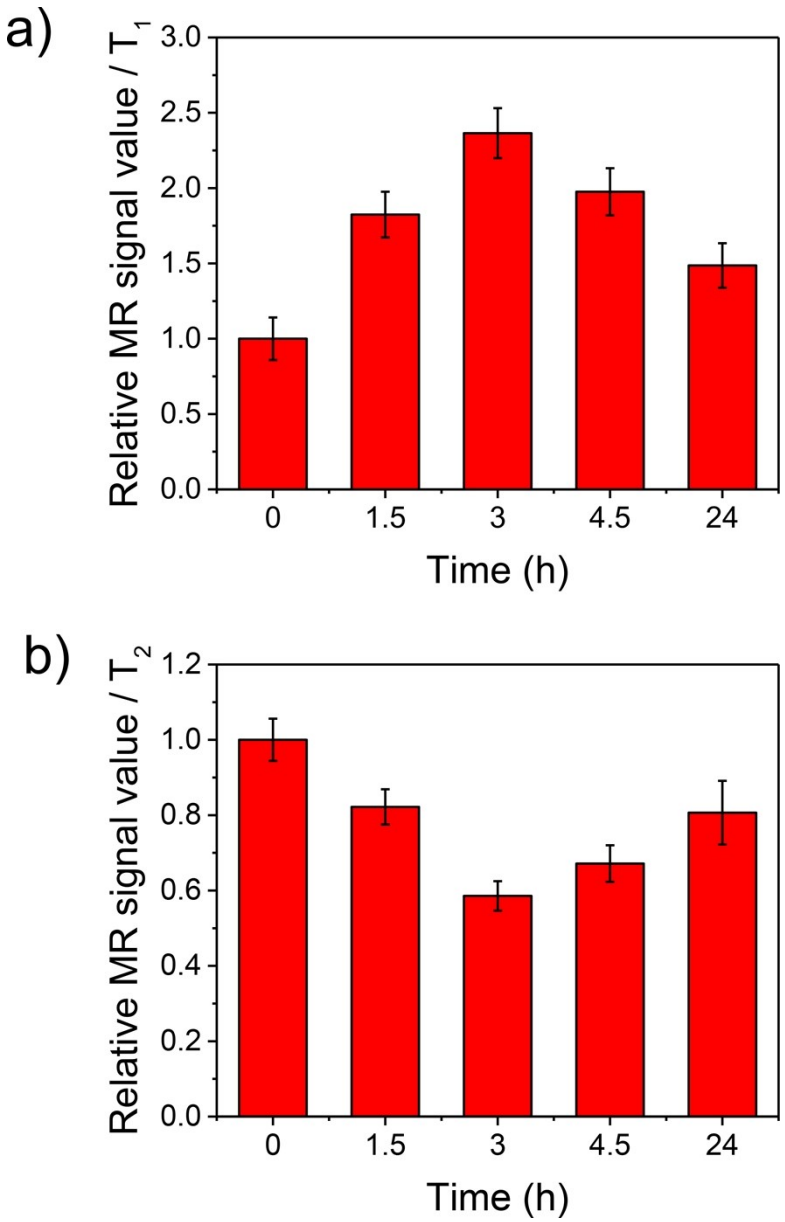

Figure S12. Relative T_1-weighted MR signal value and relative T_2-weighted MR signal value of tumor after intravenous injection of Au-Fe_3O_4@PDA-PEG-DTPA-Gd at different time intervals (0, 1.5, 3, 4.5 and 24 h). Error bars mean standard deviations (n=3).

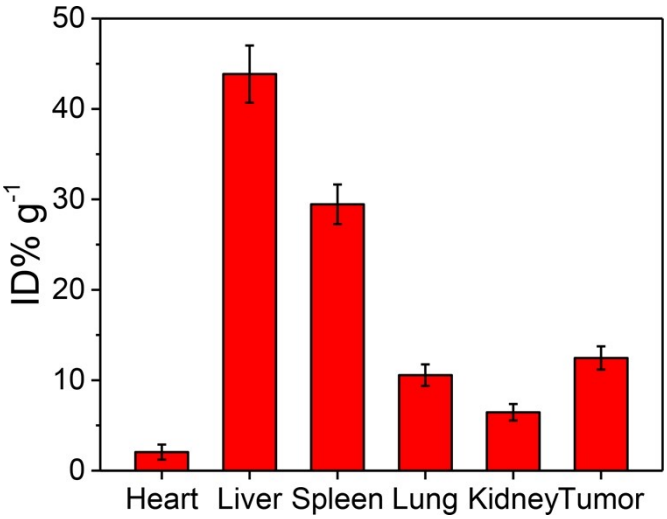

Figure S13. ICP-AES analysis of Gd element in major organs of MDA-MB-231 tumor bearing mice at 3 h post injection of Au-Fe_3O_4@PDA-PEG-DTPA-Gd. Error bars mean standard deviations (n=3)

3. Additional Table S1

Table S1. Hematology analysis of health mice treated with 0.9% NaCl solution, Au-Fe_3O_4@PDA-PEG or Au-Fe_3O_4@PDA-PEG-DTPA-Gd at 30 days post-injection.

Hematological	Units	0.9% NaCl	Au-Fe_3O_4@PDA-PEG	Au-Fe_3O_4@PDA-PEG-DTPA-Gd
WBC	$\times 10^9$/L	10.24 ± 0.22	10.22 ± 0.25	10.31 ± 0.35
RBC	$\times 10^{12}$/L	9.89 ± 0.23	9.93 ± 0.32	9.74 ± 0.46
HGB	g/L	160.46 ± 5.26	162.58 ± 3.81	165.81 ± 4.58
HCT	L/L	40.42 ± 3.12	39.5 ± 1.54	38.8 ± 2.29
RDW-CV	%	14.5 ± 0.84	13.9 ± 0.56	14.2 ± 0.71
MCH	pg	18.6 ± 0.93	19 ± 0.84	18.2 ± 0.75
MCHC	g/L	359 ± 10.51	366 ± 8.32	348 ± 9.35
MCV	fL	55.9 ± 2.86	54.9 ± 1.93	57.7 ± 2.69
PLT	$\times 10^9$/L	876 ± 15.23	842 ± 18.15	859 ± 20.35
PDW	fL	9.0 ± 0.32	9.6 ± 0.55	8.8 ± 0.44

4. Additional Reference

S1. S. Peng, Y. M. Lee, C. Wang, H. F. Yin, S. Dai and S. H. Sun, *Nano Res.*, 2008, **1**, 229-234.

S2. J. Park, K. J. An, Y. S. Hwang, J. G. Park, H. J. Noh, J. Y. Kim, J. H. Park, N. M. Hwang and T. Hyeon, *Nat. Mater.*, 2004, **3**, 891-895.

S3. F. H. Lin, H. H. Peng, Y. H. Yang and R. A. Doong, *J. Nanopart. Res.*, 2013, **15**, 13.

S4. F. H. Lin and R. A. Doong, *J. Phys. Chem. C*, 2011, **115**, 6591-6598.